CHEMISTRY OF MATERIALS

pubs.acs.org/cm

Article

Ground- and Excited-State Properties of Charged Non-Stoichiometric Quantum Dots

Omolola Eniodunmo, Shriya Gumber, Oleg Prezhdo, Dibyajyoti Ghosh, Sergei A. Ivanov, Svetlana Kilina,* and Sergei Tretiak*

Cite This: *Chem. Mater.* 2024, 36, 146−156

Read Online

ACCESS | Metrics & More | Article Recommendations | Supporting Information

ABSTRACT: Charged excited states can accumulate on the surface of colloidal quantum dots (QDs), affecting their optoelectronic properties. In experimental samples, QDs often have non-stoichiometric structures, giving rise to cation-rich and anion-rich nanostructures. We explore the effect of charge on the ground- and excited-state properties of CdSe non-stoichiometric QDs (NS-QDs) of ∼1.5 nm in size using density functional theory calculations. We compare two cases: (i) NS-QDs with a charge introduced by direct hole or electron injection and (ii) neutral NS-QDs with one removed surface ligand (with a dangling bond). Our calculations reveal that a neutral dangling bond has an effect on the electronic structure similar to that of the electron injection for the Cd-rich NS-QDs or hole injection for the Se-rich NS-QDs. In Cd-rich structures, either the injection of an electron or the removal of a passivating ligand results in the surface-localized half-filled trap state inside the energy gap. For Se-rich structures, either the injection of a hole or the removal of a ligand introduces surface-localized unoccupied trap states inside the energy gap. As a result, the charge localization formed by these two approaches leads to an appearance of low-energy electronic transitions strongly red-shifted from the main excitonic band of NS-QDs. These transitions related to a negative charge or a dangling bond exhibit weak optical activity in Cd-rich NS-QDs. Transitions related to a positive charge or a dangling bond are optically forbidden in Se-rich NS-QDs. In contrast, electron injection in Se-rich NS-QDs strongly increases the optical activity of the lowest-red-shifted charge-originated states.

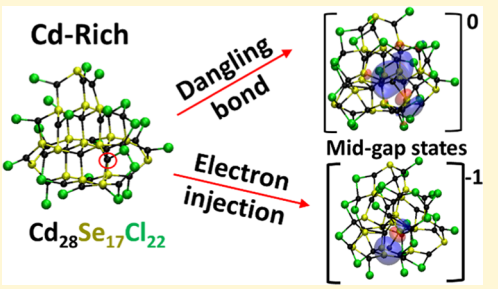

1. INTRODUCTION

Highly reproducible solution-based synthesis, long-term photostability, and easily tunable photophysical properties[1] make colloidal II−VI semiconductor quantum dots (QDs) promising for various applications ranging from photocatalysis[2] and chemical sensing[3,4] to bioimaging[5] and quantum computing.[6,7] At an atomistic scale, QDs have an inner core with a crystal structure of the bulk semiconductor, while their surface is covered by a layer of organic ligands or another semiconducting material.[8] Typically, surface ligands suppress the trap states and improve optical functionality of QDs.[9,10] In addition, surface ligands control the crystal structure of the QDs[11] and their stoichiometry.[12,13] In particular, anionic ligands have been found to stabilize non-stoichiometric compositions of QDs (NS-QDs) where the cation/anion ratio deviates from unity.[14,15] It was shown that CdSe(S) NS-QDs with the cation/anion ratio above unity (Cd-rich) are more optically active compared to those with that below unity (Se- or S-rich).[16,17] Overall, NS-QDs have exhibited improved properties critical for photocatalytic[18] and optoelectronic[19,20] applications compared to their stoichiometric counterparts. However, the photophysical properties and photoexcited dynamics of NS-QDs are sensitive to charges typically accumulating at the QD surface. Charged states commonly occur both in spectroscopic studies of QDs and during the operation of QD-based electrically driven devices.[21,22]

While the effect of stoichiometry and related surface ligands on optical properties of NS-QDs has been extensively studied both experimentally[14−17] and computationally,[23−25] the role of an excessive charge is much less investigated in NS-QDs. Several calculations based on density functional theory (DFT) have been recently reported studying the effect of various ligands and solvents on the reduction of surface metal in negatively charged cadmium chalcogenide NS-QDs.[26,27] However, these calculations do not include the characterization of the electronically excited states. Joined experimental and computational investigations of the optical response of positively charged non-stochiometric CdSe nanostructures have been reported for small clusters of 6−8 atoms in size generated by a pulsed laser vaporization source and detected with time-of-flight mass spectrometry.[28] Quenching of the

Received: June 7, 2023
Revised: December 10, 2023
Accepted: December 11, 2023
Published: December 26, 2023

Table 1. Structures of Modeled Cd-rich and Se-Rich NS-QDs Optimized in an Acetone Solvent[a]

	Neutral fully passivated	Dangling Bond DB_L	Dangling Bond DB_S	Injected Electron	Injected Hole
Cd-rich	Cd-0	Cd-1	Cd-2	Cd-0$^{(-)}$	Cd-0$^{(+)}$
Se-rich	Se-0	Se-1	Se-2	Se-0$^{(-)}$	Se-0$^{(+)}$

[a]The notations **Cd-0** and **Se-0** correspond to fully passivated neutral $Cd_{28}Se_{17}Cl_{22}$ and $Cd_{17}Se_{28}H_{22}$, respectively. The surface atom from which a ligand is removed to create a dangling bond is marked by a circle, with red circles representing the sites with the longest Cd−Cl (a solid circle) and Se−H (a dashed circle) bonds (DB_L) and blue circles showing the shortest Cd−Cl (a solid circle) and Se−H (a dashed circle) bonds (DB_S). **Cd-1** and **Se-1** represent neutral structures with dangling bonds DB_L, and **Cd-2** and **Se-2** represent neutral structures with dangling bonds DB_S for Cd-rich and Se-rich NS-QDs, respectively. **Cd-0**$^{(-)}$ and **Se-0**$^{(-)}$ are structures derived from Cd-0 and Se-0, respectively, with −1 charge (injected electron), and **Cd-0**$^{(+)}$ and **Se-0**$^{(+)}$ are the respective structures with +1 charge (injected hole).

emission upon irradiation was detected for CdSe NS-QDs of 0.7−2 nm in size and assigned to the photoinduced charging of the NS-QDs surface ligands.[29] However, the mechanisms of such photoinduced charging and the role of perfect vs imperfect ligand passivation in this process are still unclear.

A strong quantum confinement resulting from a smaller size of a QD than its exciton Bohr radii leads to relatively strong electron−hole interactions, which increases excitonic effects upon photoexcitation.[30,31] It was shown that excitons in QDs may form three-body bound states—charged excitons or trions—when paired with an additional electron (X^-) or a hole (X^+).[32−34] The presence of trions as the charged optical excitons in QDs has attracted growing interest in their potential applications for quantum information science, single photon emitters, optoelectronic devices, and quantum information technology.[6,35] In bulk semiconductors, an electric charge can be deliberately introduced by a substitution of a few atoms in the crystal lattice with impurity atoms, resulting in p- or n-doping.[20] However, this approach is more challenging for colloidal QDs.[36] On the other hand, a charge may appear naturally in the NS-QDs due to a loss or addition of one or a few ligands at the surface, forming dangling bonds.[27,37] However, it is not entirely apparent how the electronic structure and optical properties are affected by the dangling bonds and whether these changes in the ligand shell correspond to those observed for a direct electron or hole injection into the NS-QDs in photoelectrochemical experiments.[38]

In this computational study, we compare NS-QDs with a charge introduced via electron or hole injection and neutral NS-QDs with a dangling bond formed by the removal of a ligand and investigate how their ground- and excited-state properties change due to the presence of a charge or a dangling bond. Our calculations reveal that the charge-neutral system with a dangling bond has photophysical behavior similar to that of a related charged system. We consider two models of CdSe NS-QDs of about 1.5 nm in diameter: Cd-rich QDs with chloride ions used as passivating ligands to balance the excess of cations ($Cd_{28}Se_{17}Cl_{22}$) and Se-rich QDs with protons attached to selenium sites at the surface to balance excess of anions ($Cd_{17}Se_{28}H_{22}$). The fully passivated neutral $Cd_{28}Se_{17}Cl_{22}$ and $Cd_{17}Se_{28}H_{22}$ are used as reference models and labeled as **Cd-0** and **Se-0**, respectively, as illustrated in Table 1. These NS-QD models have similar structures as those computationally studied in refs 24,39. An analogous model with a larger size $Cd_{68}Se_{55}Cl_{26}$ has also been investigated in refs 26,27.

It is important to note that while organic ligands are commonly used for surface passivation of QDs, chloride passivation (X-type ligands) of CdSe QDs have been proven as an alternative for reducing surface defects, controlling surface trapping, and enhancing photocurrent and photocatalytic activity.[40−42] Thus, our Cl-passivated Cd-rich structures provide a model case of real NS-QD samples used in experiments.[38] Synthesis, structure characterization, and optical properties of Se-rich NS-QDs of size from 0.7 to 2 nm with selenophenol passivating ligands have been previously reported,[29] which we consider as analogues for our H-passivated Se-rich models. For computational efficiency, we further replace the phenyl substituents with H, as it is commonly done in molecular modeling.[30,31]

1.1. Models of NS-QDs with a Charge Introduced via a Dangling Bond or an Electron/Hole Injection. We introduce a dangling bond at the surface of the NS-QD **Cd-0** (**Se-0**) by removing Cl (H) capping ligands contributing either to the longest (and weakest) Cd−Cl (Se−H) bond, DB_L, or to the shortest (and strongest) Cd−Cl (Se−H) bond, DB_s, as shown in Table 1. We use notations **Cd-1** and **Se-1** for structures with DB_L and **Cd-2** and **Se-2** for structures with DB_S for Cd-rich and Se-rich NS-QDs, respectively. It is reasonable to assume that an ion (either Cl^- or H^+) can leave the surface, resulting in the unbalanced charge of the NS-QD, with +1 charge on Cd-rich structures **Cd-1**$^{(+)}$ and **Cd-2**$^{(+)}$ or −1 charge on Se-rich structures **Se-1**$^{(-)}$ and **Se-2**$^{(-)}$. However, such charged structures are not likely to survive in a solution for a long time without being neutralized by the same ion or by another charge exchange with the environment (e.g., via molecular oxygen or surface electrochemical reactions),[43] stabilizing the incompletely passivated NS-QDs.[44,45] Alternatively, charging of NS-QDs could force X-type (donor-type) ligands off the surface to retain charge neutrality while resulting in an imperfect surface passivation.[46] As such, we mainly focus

https://doi.org/10.1021/acs.chemmater.3c01414
Chem. Mater. 2024, 36, 146−156

on neutral structures with DB_L (**Cd-1** or **Se-1**) and DB_S (**Cd-2** or **Se-2**) dangling bonds. The notations **Cd-0**$^{(-)}$ and **Se-0**$^{(-)}$ represent fully passivated structures of **Cd-0** and **Se-0**, respectively, charged negatively via an electron injection, and **Cd-0**$^{(+)}$ and **Se-0**$^{(+)}$ are their counterparts positively charged via the hole injection into **Cd-0** and **Se-0**, respectively (Table 1). Scheme 1 illustrates the considered cases obtained from neutral **Cd-0** and **Se-0** via either charge injection or ligand removal.

Scheme 1. Schematics of Modeled Structures with a Charge and Dangling Bonds from Original Cd-rich NS-QD, $Cd_{28}Se_{17}Cl_{22}$ (Cd-0); Se-Rich Analogues Can be Obtained by Switching Places of Cd and Se Symbols and Replacing Cl with H

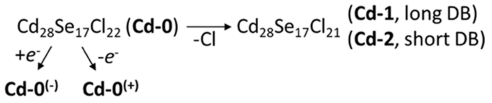

2. RESULTS AND DISCUSSION

2.1. Ground-State Electronic Structure: Charge-Related Midgap States. An extra charge introduced via the direct electron/hole injection creates an odd number of electrons in the system, resulting in a doublet spin multiplicity of the ground state. Similarly, the removal of one chlorine or hydrogen (both having an odd number of electrons) also leads to a doublet spin multiplicity of the ground state for the NS-QDs with a dangling bond while retaining charge neutrality. The optimized geometries of all constructed NS-QD models calculated in vacuum and acetone at the spin-unrestricted DFT level are represented in Figure S1 in the Supporting Information (SI). The computational methodology details are provided in the Section 4. To understand the difference in the electronic structure introduced by the electron/hole injection and dangling bonds, Figures 1 and 2 show the spin-polarized projected density of states (PDOS) and frontier orbitals (insets) calculated for considered cases of Cd-rich and Se-rich NS-QDs, respectively.

For Cd-rich NS-QDs, the electronic structure of **Cd-0**$^{(-)}$ resulting from electron injection (Figure 1b) looks qualitatively similar to that of neutral **Cd-1** featuring dangling bonds (Figure 1a). The dangling bond site, the location of the Cd−Cl bond removal, does not change this trend, as evident in Figure S2, where the PDOS of **Cd-1** and **Cd-2** are compared. The electronic structures of **Cd-0**$^{(-)}$ and **Cd-1** (**Cd-2**) show a midgap state (HOMO) occupied with a single spin-up electron localized on a few surface cadmium sites with a relatively small contribution from the neighboring seleniums (insets of Figure 1a,1b). This result correlates with the spectroelectrochemical signatures of Cd-localized trap states within the band gap experimentally detected in CdTe NS-QDs with the surface treated by different metal chloride salts.[43] The similarity in the electronic orbitals between the NS-QDs with a dangling bond and an injected electron can be explained by the following factors. Upon electron injection into **Cd-0**, the electron occupies the LUMO of the neutral NS-QD, which is mainly distributed over the cadmium sites (Figure S2a). However, occupation of this orbital by an added electron leads to the stabilization of the former and shifting its energy inside the band gap, thereby forming new HOMO of **Cd-0**$^{(-)}$ and leading to a strong localization of the electron density around a few surface cadmiums, as illustrated in the inset of Figure 1b. For comparison, the PDOS and frontier orbitals of the neutral **Cd-0** structure are shown in Figures S2b and S3b.

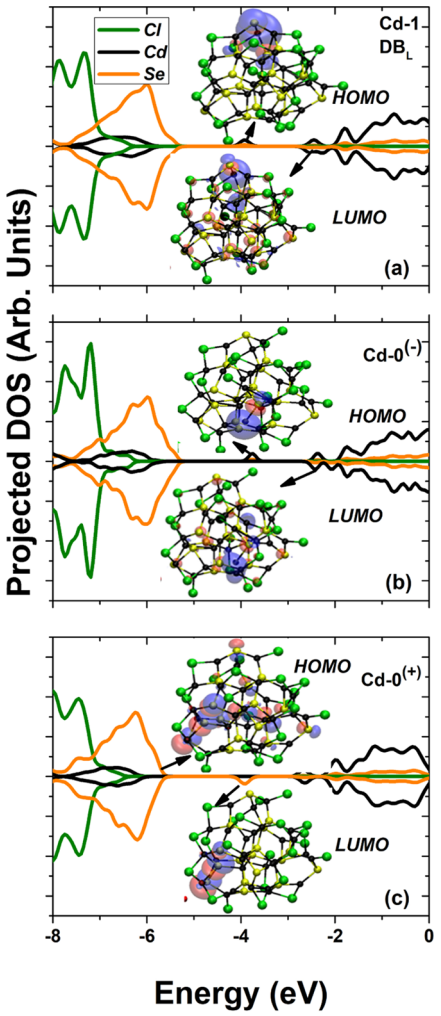

Figure 1. Spin-polarized projected density of states (PDOS) and ground-state frontier molecular orbitals for Cd-rich NS-QDs with a dangling bond and an injected electron/hole calculated in acetone. (a) **Cd-1** structure with DB_L dangling bond (Cl ligand is removed from the longest Cd−Cl bond); (b) **Cd-0**$^{(-)}$ structure with an injected electron; and (c) **Cd-0**$^{(+)}$ structure with an injected hole. The up and down arrows denote the highest occupied molecular orbital (HOMO) and lowest unoccupied molecular orbital (LUMO), respectively, with their images shown in insets.

The highly Cd-localized character of HOMO associated with a negative charge is also supported by the idea that a charge density of an added electron is expected to be located around the most positively charged sites on the QD surface. Therefore, the HOMO of **Cd-0**$^{(-)}$ (inset of Figure 1b) is mainly localized on a few surface cadmiums with the lowest partial positive charges. Likewise, in neutral **Cd-1** (inset of Figure 1a) and **Cd-2** (inset of Figure S2c), the presence of dangling bonds results in the electronic density of HOMO distributed around the cadmium with lost chlorine to make it less electropositive. This trend (i.e., gaining less positive charge on the surface cadmiums contributing to the dangling bonds compared to those of the fully passivated **Cd-0** structure) is evident from the analysis of natural bond orbitals (NBO) presented in Table S1. This behavior is accommodated by

https://doi.org/10.1021/acs.chemmater.3c01414
Chem. Mater. 2024, 36, 146−156

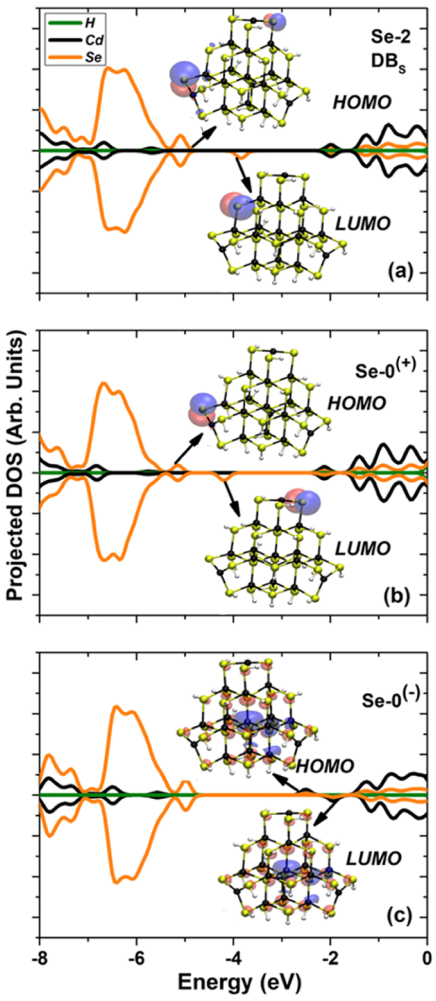

Figure 2. Spin-polarized projected density of states (PDOS) and ground-state frontier orbitals for Se-rich NS-QDs with injected electron/hole and dangling bonds calculated in acetone. (a) **Se-2** structure with DB_S dangling bond (H ligand is removed from the shortest Se−H bound); (b) **Se-0**$^{(+)}$ structure with injected hole, and (c) **Se-0**$^{(-)}$ structure with injected electron. The up and down arrows denote the HOMO and LUMO, respectively, with their images shown in insets.

reducing the distance between cadmium sites on which the electron density is localized compared to those of the **Cd-0** structure. While less pronounced in larger systems, this trend agrees with reported surface reconstruction in the $Cd_{68}Se_{55}Cl_{26}$ model with imperfect surface passivation resulting in Cd−Cd dimers, which manifest themselves as charge traps within the band gap.[27]

As can be seen in Figure 1a,b, for both **Cd-1** and **Cd-0**$^{(-)}$, the LUMO is distinct in energy from the rest of the conduction band, while its charge density (insets of Figure 1a,b) is highly delocalized over the entire system similarly to those of the fully passivated **Cd-0** structure shown in insets of Figure S2a and S3b. This trend is independent of the location of the dangling bond showing comparable behavior of LUMO for both **Cd-1** and **Cd-2** structures (Figure S2a−c). Similar electron delocalization at the edge of the conduction band has been observed in larger models of fully passivated $Cd_{68}Se_{55}Cl_{26}$, where the electron injection into the system occurs upon addition of a potassium atom on the surface.[26,27] Overall, we conclude that losing a ligand from the surface of a Cd-rich NS-QD results in the electron doping of the system, similar to the direct electron injection.

In contrast, the positive charge contributed from hole injection in **Cd-0**$^{(+)}$ (Figure 1c) is different in its impact on the electronic structure compared to the systems with dangling bonds, **Cd-1** (Figure 1a) and **Cd-2** (Figure S2c). The structure **Cd-0**$^{(+)}$ features an unoccupied midgap state (LUMO) localized over a few closely located selenium sites, while the HOMO is noticeably delocalized over the entire system, with its energy being at the edge of the valence band (inset of Figure 1d). The nature of Se-localized LUMO of **Cd-0**$^{(+)}$ is caused by hole injection from **Cd-0** leading to the vacant HOMO of **Cd-0**, which is originated mainly from seleniums (inset of Figure S2a) while destabilizing its energy and shifting it inside the energy gap resulting in the partially unoccupied midgap state. It is important to note that the introduced positive charge in **Cd-0**$^{(+)}$ gives rise to a drastically different effect on the electronic structure when compared not only to the neutral **Cd-1** and **Cd-2** with dangling bonds but also to the positively charged **Cd-1**$^{(+)}$ and **Cd-2**$^{(+)}$ with one lost Cl^- anion, as shown in Figure S2d−f. The positively charged structures with one lost surface ion, **Cd-1**$^{(+)}$ and **Cd-2**$^{(+)}$, do not possess Cd-localized midgap hole trap states, like neutral **Cd-1** (Figure S1a) and **Cd-2** (Figure S2d), or Se-localized midgap electron trap states like **Cd-0**$^{(+)}$ (Figure 1c). Instead, loss of Cl^- surface ion results in shallow hole trap states localized on a few Se sites (Figure S2e,f) similar to those observed in the stoichiometric $Cd_{33}Se_{33}$ with imperfect surface passivation by L-type pyridine, amine, or phosphine oxide ligands.[47]

Figure 2 compares the spin-polarized PDOS of the charged Se-rich NS-QDs. In this case, the ground-state electronic structure of **Se-0**$^{(+)}$ with an injected hole (Figure 2b) is quite similar to those of neutral structure **Se-2** with a dangling bond generated via loss of hydrogen from the surface (Figure 2a). The location of the Se−H bond removal does not affect this trend, as evidenced from a comparison of the PDOS of **Se-2** and **Se-1** structures in Figure S4b,c. For all of these cases, the unoccupied midgap state (LUMO) is strongly localized on surface selenium (insets of Figures 2a,b and S4c). The Se-localized nature of the LUMO of **Se-0**$^{(+)}$ originates from a hole injection to the HOMO of the neutral **Se-0** system, which is localized around a few electron-rich selenium sites at the surface (Figures S4a and S5b). Similarly, for neutral **Se-2** and **Se-1**, a dangling bond originated from a loss of hydrogen coordinated to selenium creates a surface defect localizing the LUMO around this selenium (insets of Figures 2b and S4c).

Comparing the charge on the selenium contributing to the dangling bond in **Se-1** and **Se-2** to those of the neutral but fully passivated **Se-0** system, we observe that losing hydrogen makes this Se less negative, Table S1. The trend in reducing the absolute value of the negative charge on selenium with removed hydrogen supports similarities in the electronic structure between the cases of an injected hole in **Se-0**$^{(+)}$ and dangling bonds in neutral **Se-1** and **Se-2**. It is worth noting that the charge localization, calculated based on the natural orbital analysis, is consistent with spin density plots presented in Table S2 in the SI.

For the **Se-0**$^{(-)}$ structure, an electron is expected to be added to the LUMO of the neutral **Se-0** system associated with an electron-deficient cadmium (Figure 4Sa), stabilizing its energy and shifting new HOMO of **Se-0**$^{(-)}$ inside the energy gap, Figure 2c. Since Se-rich structures have cadmiums at the

https://doi.org/10.1021/acs.chemmater.3c01414
Chem. Mater. 2024, 36, 146−156

core rather than at the surface, the HOMO of **Se-0**$^{(-)}$ is distributed mainly over cadmium sites in the inner part of the NS-QD with some contributions from surface seleniums (insets of Figure 2c). Thus, electron injection in **Se-0**$^{(-)}$ leads to the delocalized nature of the HOMO with significant contributions from core cadmiums. The LUMO of **Se-0**$^{(-)}$ also has a highly delocalized nature with significant contributions from core cadmiums (insets of Figure 2c).

The discussed trends in the electronic structure for both Cd-rich and Se-rich NS-QDs with injected electron/hole and dangling bonds are qualitatively consistent in polar media and a vacuum, as shown in Figures S3 and S5. Noteworthy, the delocalized nature of HOMO and LUMO due to electron injection in **Se-0**$^{(-)}$ (Figure 2c) is very different compared to that in **Cd-0**$^{(-)}$, where the LUMO exhibits delocalized character, but the HOMO is localized on a few surface cadmiums (Figure 1a). The electronic structure of negatively charged **Se-0**$^{(-)}$ is also different from those of negatively charged **Se-1**$^{(-)}$ and **Se-2**$^{(-)}$, where a surface proton has been removed, Figure S4d–f. Negatively charged **Se-1**$^{(-)}$ and **Se-2**$^{(-)}$ structures with imperfect surface passivation just have more Se-localized hole trap states at the edge of the valence band, while their conduction bands remain unchanged (Figure S4e,f), compared to the neutral fully passivated **Se-0** (Figure S4a).

Overall, imperfectly passivated Cd-rich and Se-rich NS-QDs with a charge introduced by losing one of the surface ligands in their ionic form demonstrate shallow hole trap states near the edge of the valence band, which are comparable to those of the neutral stochiometric QDs with a removed L-type pyridine, amine, or phosphine oxide ligand.[47] In contrast, dangling bonds in the neutral NS-QDs result in effects on the electronic structure comparable to those of the charged fully passivated NS-QDs: half-filled midgap states appear with a strong localization on a few surface cadmiums in **Cd-0**$^{(-)}$ and **Cd-1** (**Cd-2**) or with a strong localization on a few surface seleniums in **Se-0**$^{(+)}$ and **Se-1** (**Se-2**). Because of this similarity, we refer to these systems as "charged" structures, where a charge is introduced either directly via electron or hole injection (**Cd-0**$^{(-)}$ and **Se-0**$^{(+)}$) or via the generation of neutral dangling bonds (**Cd-1**/**Cd-2** and **Se-1**/**Se-2**), respectively.

2.2. Excited-State Calculations: Charge-Related Optical Transitions. Figure 3 shows the absorption spectra of considered NS-QDs calculated in acetone using the TDDFT method. For comparison, absorption spectra for these systems computed in vacuum are shown in Figure S6, demonstrating trends similar to those in the polar media. For Cd-rich structures, a localized charge introduced either directly via electron or hole injection (**Cd-0**$^{(-)}$ and **Cd-0**$^{(+)}$) or via the generation of dangling bonds in neutral systems (**Cd-1** and **Cd-2**) results in optically weak (**Cd-1**, **Cd-2**, and **Cd-0**$^{(-)}$) or completely optically forbidden (**Cd-0**$^{(+)}$) lowest-energy transitions at the range of 0.7–1.3 eV. These transitions are significantly red-shifted with respect to the first absorption peak of the neutral, fully capped **Cd-0** structure, Figure 3a. In the spectroelectrochemical measurements, a similar red-shifted optically weak absorption feature has been detected under the applied negative voltage for CdTe NS-QDs with chloride capping, which is attributed either to a Stark shift or a trion shift.[43] In **Cd-0**, the first absorption peak appears around 2.9 eV, manifesting the highly intensive lowest excitonic state (magenta line in Figure 3a). Similar absorption bands at this energy range are also well pronounced in all Cd-rich systems

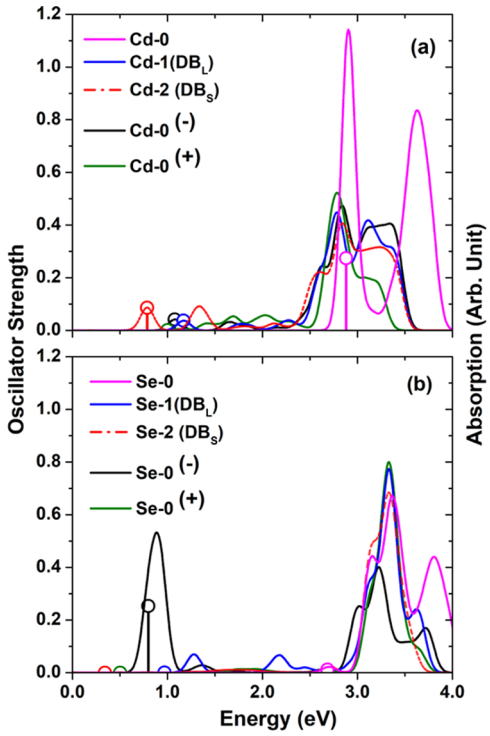

Figure 3. Absorption spectra of NS-QDs in question calculated in acetone. (a) Cd- and (b) Se-rich structures. The vertical lines with circles represent the lowest optical transitions for each considered structure. The height of the vertical line corresponds to the oscillator strength of each transition. When semicircles are shown, the corresponding electronic transition is optically inactive.

with the introduced charge (Figure 3a). This highly intensive "bright" peak can be assigned to a neutral exciton, which qualitatively agrees with experimental data.[33]

For neutral **Cd-1** and **Cd-2** structures and charged **Cd-0**$^{(-)}$ dot, the red-shifted optically weak states appearing around 0.7–1.3 eV are induced by the localized charge density on the half-filled frontier orbital (related to −1 charge) in the presence of the lowest bright exciton (~2.9 eV). We rationalize weak optical intensities of the calculated lowest-energy optical transitions related to the negative charge by the highly localized nature of their hole density distribution, as evidenced from natural transition orbitals (NTOs), compared to the delocalized NTOs of neutral excitons in the fully capped **Cd-0** system, Table 2. The localized nature of the hole contributing to the lowest optical transition of these red-shifted states in charged Cd-rich systems is consistent with their ground-state HOMO localized on surface cadmiums (Figure 1a,b). Similar trends in NTO distributions are found for all Cd-rich structures calculated in a vacuum, Table S3. These charge-related states can be compared to the negative trion X^- states, which are identified as red-shifted states with weak optical activity observed during the electron injection in CdSe/CdS core/shell QDs.[33,48] A noticeable optical intensity of red-shifted X^- trions have also been detected in charged CdSe/ZnS and CdTe/CdSe core/shell QDs.[49,50]

Notably, the lowest-energy transition in **Cd-0**$^{(+)}$ structure is optically forbidden (green line in Figure 3a) due to the highly surface-localized nature of both the electron and the hole contributing to this state, Table 2. These results agree with both experimental and calculated absorption spectra of small positively charged Cd_4Se_3 clusters demonstrating the appear-

https://doi.org/10.1021/acs.chemmater.3c01414
Chem. Mater. 2024, 36, 146–156

Table 2. Natural Transition Orbitals (NTOs) Depicting the Electron−Hole Pairs with Different Spin Components Contributing to the First Optical Transition of Absorption Spectra for Cd-Rich NS-QDs with a Charge Introduced by Electron Injection (Cd-0$^{(-)}$), Hole Injection (Cd-0$^{(+)}$), and Dangling Bonds (Cd-1 and Cd-2) and Compared to Those of the Neutral Fully Passivated Cd-0 Structure[a]

Cd-rich	Hole		Electron	
	Alpha	Beta	Alpha	Beta
Cd-0$^{(-)}$ 1.076 eV (0.04)	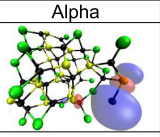	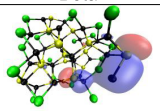	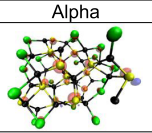	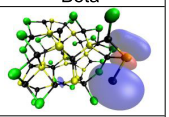
Cd-0$^{(+)}$ 1.000 eV (0.00)	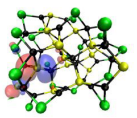	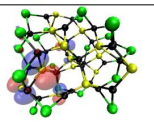	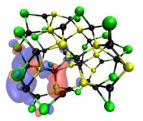	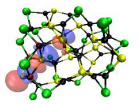
Cd-1 1.169 eV (0.04)	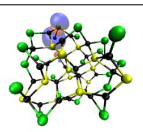	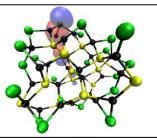	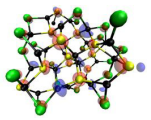	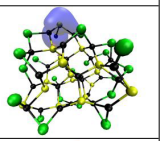
Cd-2 0.786 eV (0.09)	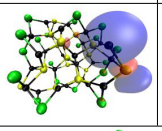	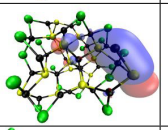	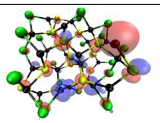	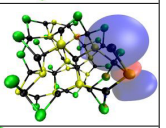
Cd-0 2.880 eV (0.27)	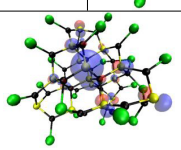		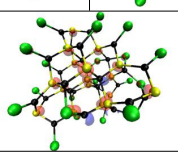	

[a]All data were calculated in an acetone environment. The transition energies are shown in eV, and the oscillator strength values are presented in parentheses.

ance of red-shifted optically inactive transitions.[28] These charge-related optical transitions can be compared to the positive trion X^+ state induced by a coupling between +1 charge and the lowest bright exciton. An optically "dark" character of the calculated transitions associated with a positive charge of Cd-rich structures is consistent with respective experimental observations for positively charged CdSe/CdS core/shell QDs: structures with injected holes show the X^+ trion state with diminishing emission intensity (the dark state), while structures with injected electrons demonstrate the X^- trion state with intermediate photoluminescence strength.[33] We note that while in the core/shell QDs, the CdS shell isolates stoichiometric CdSe core from the surface effects, an imperfect interface can give rise to the Cd-rich stoichiometry similar to our Cd-rich NS-QD models, justifying the comparison between the calculated and experimental data.

For Se-rich NS-QDs, the first absorption peak of the neutral fully passivated **Se-0** system appears around 2.7 eV, a contribution from the lowest optically weak transition, followed by an optically intensive peak at ∼3.2 eV (magenta line in Figure 3b). The energy of the first optically active band agrees well with the experimental absorption band at ∼3.4 eV reported for Se-rich NS-QDs having ∼20 cadmiums in the core, while broad, red-shifted emission at low temperatures and significantly reduced emission at room temperature with long decay times resemble the characteristics of the deep trapped emission, which arises from forbidden transitions of surface states.[12,29] We believe that the weak optical intensity of the lowest-energy state is introduced by the charge-transfer character of the lowest exciton originating from the core-localized electron and surface-localized hole, which is consistent with previously reported work.[24]

The Se-rich positively charged **Se-0**$^{(+)}$ and neutral **Se-1** and **Se-2** with dangling bonds exhibit red-shifted optically inactive states appearing at about 0.8−1.0 eV, Figure 3b. These states are associated with a strongly localized positive charge in the presence of the lowest-energy optically weak exciton, which can be compared to the positive trion X^+ states detected in electrochemically positively charged CdSe QDs.[51] Because of the highly localized character of the electron−hole pair—with both an electron and a hole located on the surface selenium atoms—this charge-related state is optically inactive for **Se-1**, **Se-2**, and **Se-0**$^{(+)}$ structures, Table 3.

The localized character of the lowest exciton is consistent with both HOMO and LUMO localized on surface seleniums for these structures (Figure 2a,b) and has a similar trend in vacuum (Table S4). In experiments, a drastic decrease of the emission intensity after illumination (photodarkening) of the Se-rich NS-QDs has been observed.[29] Irreversible photodarkening is associated with photochemical cleavage of the Se−ligand bonds, while partially reversible photodarkening is explained by temporary charging of the NS-QDs with an electron trapped on the ligand shell.[29] This observation is in agreement with our computational results. In addition, transit absorption of Se-rich NS-QDs has revealed the fraction of a surface charge understood in terms of the density of unligated surface seleniums involved in a rapid nonradiative Auger relaxation of the X^+ trion states upon photoexcitation, explaining quenched emission in Se-rich NS-QDs.[12] These experimental results qualitatively agree with our calculations, supporting our main conclusion that a dangling bond in Se-

https://doi.org/10.1021/acs.chemmater.3c01414
Chem. Mater. 2024, 36, 146−156

Table 3. NTOs Depicting the Electron−Hole Pair with Different Spin Components Contributing to the First Optical Transition of Absorption Spectra for Se-rich NS-QDs with a Charge Introduced by Electron Injection (Se-3), Hole Injection (Se-0$^{(+)}$), and Dangling Bonds (Se-1 and Se-2) and compared to Those of the Neutral Fully Passivated Se-0 Structure[a]

Se-rich	Hole		Electron	
	Alpha	Beta	Alpha	Beta
Se-0$^{(-)}$ 0.797 eV (0.25)	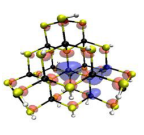		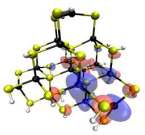	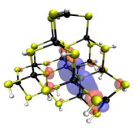
Se-0$^{(+)}$ 0.502 eV (0.00)	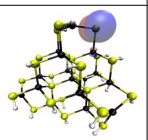	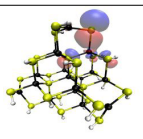	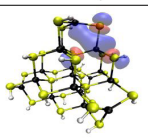	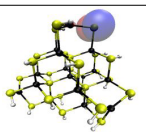
Se-1 0.968 eV (0.00)	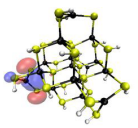	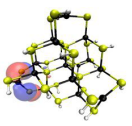	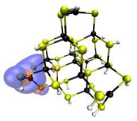	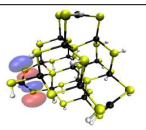
Se-2 0.341 eV (0.00)	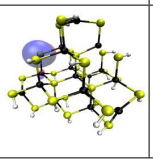	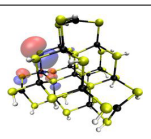	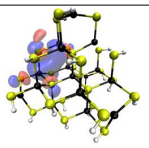	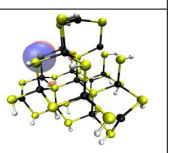
Se-0 2.685 eV (0.01)	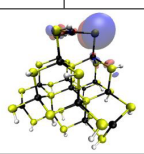		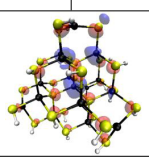	

[a]All data were calculated in an acetone environment. The transition energies are shown in eV, and the oscillator strength values are presented in parentheses.

rich QDs has similar photophysical effects as an injected hole leading to red-shifted optically inactive states.

Thus, a positive charge introduced to Se-rich NS-QDs either via direct hole injection (**Se-0**$^{(+)}$) or neutral dangling bonds (**Se-1** and **Se-2**) results in the strongly red-shifted optically dark hole-related states (Figure 3b). In contrast, extra electron presence in **Se-0**$^{(-)}$ leads to the optically active charge-related state red-shifted to ∼0.8 eV (black line in Figure 3b). This optical activity of the negative charge-associated state can be rationalized by the significantly delocalized character of the related electron−hole pair, with a predominant contribution from core cadmiums, Table 3. In accordance with our results, it was experimentally detected that negatively charged CdSe/ZnSe QDs show emitting X^- trion state at low temperatures.[52] In this core/shell structure, the interface can resemble the Se-rich non-stoichometric surface, similar to our Se-rich NS-QD models. The difference in the optical activity of the negative charge-related state between **Cd-0**$^{(-)}$ and **Se-0**$^{(-)}$ cases also agrees well with the experimentally observed emission enhancement of NS-QDs with Se-rich surfaces when electron-donor tertiary phosphine ligands are added, while these ligands have a minor effect on emission of Cd-rich structures.[53]

Strongly red-shifted optical transitions associated with a charge introduced either via direct electron/hole injection or via a dangling bond in the neutral Cd-rich and Se-rich structures differ from the lowest-energy transitions of **Cd-1**$^{(+)}$/**Cd-2**$^{(+)}$ and **Se-1**$^{(-)}$/**Se-2**$^{(-)}$ with one lost surface ion. For these charged systems with imperfect surface passivation, optically inactive transitions contributed from shallow trap states are insignificantly red-shifted with respect to the optically active first absorption band (Figure S7), showing similar absorption features as neutral stoichiometric CdSe QDs with removed L-type ligands.[47]

While the calculated optical features related to the charge/dangling bond in NS-QDs show qualitative agreement with the optical response of trion states detected in experiments,[12,33,48−52] our TDDFT calculations do not include higher-order correlations such as 3-body interactions to accurately define the trion state, where a charge is coupled to an exciton. As such, our calculations can be viewed as an approximation to a more accurate time-dependent density-matrix functional theory suggested in refs 54,55 for the treatment of trion states. This approximation seems to be appropriate for studying the qualitative behavior of X^+ and X^- trion states. We also would like to note that recent spectroelectrochemistry experiments[21,22] probing the trion state of charged CdSe QDs have shown that the additional electron in the conduction band accelerates the hot electron cooling by enhanced electron−electron scattering followed by charge redistribution and polaron formation on a picosecond time scale. After that, trions undergo decay through the Auger process within 300−500 ps, exemplifying the manifestation of a phonon bottleneck effect.[22] While our calculations do not represent a photodynamic process, the reorganization of NS-QDs geometries in the presence of a charge qualitatively represents charge−phonon interactions. More accurate simulations of these processes have been recently performed by our group for neutral **Cd-0** and **Se-0** models capped by different halide and alkali metal ligands and revealed that the size of the

https://doi.org/10.1021/acs.chemmater.3c01414
Chem. Mater. 2024, 36, 146−156

surface ligands directly affects the lattice vibrations and electron−phonon couplings. This leads to significant variations in nonradiative rates of phonon-mediated relaxation of electrons ranging from 10s to 100s ps.[39] Analogous simulations for charged Cd-rich and Se-rich structures will be the focus of our future investigations to confirm the effect of the charge on the electron cooling dynamics.

3. CONCLUSIONS

In this work, we computationally explore several different ways of introducing a surface-localized charge into the Cd-rich and Se-rich NS-QDs and reveal how these different mechanisms influence the ground- and excited-state properties of these systems. Our calculations demonstrate that imperfectly passivated Cd-rich and Se-rich NS-QDs, when charged by removing one of the surface ligands in their ionic form, exhibit relatively similar electronic structures. These structures feature shallow hole trap states near the edge of the valence band, which are comparable to those of the neutral stoichiometric QDs with a removed L-type pyridine, amine, or phosphine oxide ligand.[47] In contrast, the formation of a neutral dangling bond via the removal of a chlorine ligand from the surface of the Cd-rich NS-QD is similar to negatively charging the fully passivated system. Thus, neutral Cd-rich structures with dangling bonds (**Cd-1** and **Cd-2**) have similar changes in their electronic structure as those in the **Cd-0**$^{(-)}$ structure formed by direct electron injection. All of these structures exhibit half-filled trap states within the energy gap, which are strongly localized on a few surface cadmiums. In the case of Se-rich NS-QDs, a neutral dangling bond resulting from the loss of surface hydrogen is analogous to the positive charging of a fully passivated system. Thus, both cationic **Se-0**$^{(+)}$ and neutral **Se-1**/**Se-2** structures feature midgap electron trap states strongly localized on a few surface seleniums.

The charge localization on the surface sites of NS-QDs, through either a charge injection or a neutral dangling bond, results in strongly red-shifted optical transitions. These lowest-energy transitions can be compared to the coupled state between an optical exciton and a charge, a trion. The optical transitions related to a negative charge (or a neutral dangling bond) hold weak optical activity in Cd-rich NS-QDs, while transitions related to a positive charge (or a neutral dangling bond) in Se-rich NS-QDs have an optically dark character. The reduced optical intensity of the states associated with a positive charge/dangling bond in Se-rich structures is rationalized by a stronger spatial localization of the electron−hole pair on surface seleniums, compared to a more delocalized character of an electron contributing to the states related to a negative charge/dangling bond in Cd-rich systems. The positive charge-related state in Cd-rich NS-QDs with an injected hole is also completely optically inactive due to the highly surface-localized nature of both the electron and the hole contributing to this state. In contrast to Cd-rich NS-QDs, electron injection in a Se-rich QD creates an optically active charge-related state with a highly delocalized nature of its electron−hole pair over the core cadmiums. Thus, our calculations predict that the lowest optically weak or inactive states in Se-rich NS-QDs can be "brightened" by introducing a negative charge to the system, creating an optically active trion X^- state that is red-shifted with respect to the main excitonic band. Overall, our results provide valuable insights into the mechanisms of controlling the optical activities of the lowest-energy states in QDs through their stoichiometry, surface ligands, and charges.

4. COMPUTATIONAL METHODS

Calculations are performed at the level of the DFT, as implemented in the Gaussian-16 software package.[56] The ground-state geometries and the electronic structure of the NS-QD structures are optimized using hybrid density functional B3LYP[57] and a mixed basis set of LANL2DZ[58] for Cd and Se atoms and 6-31-G*[59] for H and Cl atoms. For all calculations with an odd total number of electrons, spin-unrestricted calculations were carried out. This allows the spin-up (α) and spin-down (β) orbitals to relax independently from each other, resulting in two distinct densities of states that are shown above (α) and below (β) the x-axis in Figures 1 and 2, showing the projected DOS of considered structures.

The excited-state calculations are carried out with the linear response time-dependent DFT (TDDFT) methodology using the same density functional model and basis set as those for the ground-state calculations. The TDDFT calculations yield the transition density matrix, from which the energy and the oscillator strength of each electronic transition are obtained, as implemented in the Gaussian-16 software package. To simulate the absorption spectra, the 150 lowest singlet transitions are calculated to reach the 4.5 eV spectral range. These transitions are broadened by a Gaussian function with a line width of 0.1 eV to represent thermal line-broadening at ambient conditions.

The nature of excited states is characterized by natural transition orbitals (NTOs)[60] representing the spatial distribution of the electron−hole pair contributing to each optical transition. NTOs for the lowest-energy transitions have been visualized using the isosurface value of 0.02, which is a typical threshold value for the isodensity surfaces to clearly represent the spatial distribution of electron and hole density in molecules and nanostructures.[61] The 3-D graphical images of NTOs are plotted using VMD-1.9.3 software.[63] Both ground-state and excited-state calculations for all NS-QD structures are performed in vacuum and acetone; for the solvent effects, the conductor-like polarizable continuum model (CPCM)[64] is used. Overall, the applied computational methodology has been thoroughly tested and used for a wide variety of previously modeled stoichiometric[47,65,66] and non-stoichiometric QDs.[24,28]

We note that quantitative calculations of trion states, where the charge is coupled to a neutral exciton, require explicit inclusion of three-body interactions, which are not present in the TDDFT. A more accurate approach based on time-dependent density-matrix functional theory (TD-DMFT) for calculating trions in nanostructures has been utilized in refs 54−62. Our approach can be considered as an approximation to this method, where the trion state is considered in the noninteracting basis of an electron (a hole) and an exciton.

■ ASSOCIATED CONTENT

Supporting Information

The Supporting Information is available free of charge at https://pubs.acs.org/doi/10.1021/acs.chemmater.3c01414.

Natural ond orbitals comparing the charge on the selected Cd and Se bonded to Cl or H ligands; spin density and natural orbitals for charged Cd-rich and Se-rich structures calculated in acetone; optimized geometries of all studied NS-QDs calculated in vacuum and in acetone; spin-polarized projected density of states and ground-state molecular orbitals for Cd-rich and Se-rich NS-QDs calculated in vacuum; absorption spectra for Cd-rich and Se-rich structures in vacuum; natural transition orbitals presenting the electron−hole pair contributing to the first optical transition in Cd-rich and Se-rich NS-QDs calculated in vacuum; the xyz coordinates of **Cd-0**, **Cd-1**, and **Cd-2** (neutral and with +1 charge), **Cd-0**$^{(-)}$ and **Cd-0**$^{(+)}$ for Cd-rich, and analogous Se-rich structures optimized in acetone (PDF)

https://doi.org/10.1021/acs.chemmater.3c01414
Chem. Mater. 2024, 36, 146−156

AUTHOR INFORMATION

Corresponding Authors

Svetlana Kilina − *Department Chemistry and Biochemistry, North Dakota State University, Fargo, North Dakota 58108, United States;* orcid.org/0000-0003-1350-2790; Email: svetlana.kilina@ndsu.edu

Sergei Tretiak − *Materials Physics and Applications Division and Center for Integrated Nanotechnologies and Theoretical Division, and Center for Nonlinear Studies Los Alamos National Laboratory, Los Alamos National Laboratory, Los Alamos, New Mexico 87545, United States;* orcid.org/0000-0001-5547-3647; Email: serg@lanl.gov

Authors

Omolola Eniodunmo − *Department Chemistry and Biochemistry, North Dakota State University, Fargo, North Dakota 58108, United States*

Shriya Gumber − *Department of Chemistry and Department of Physics and Astronomy, University of Southern California, Los Angeles, California 90089, United States*

Oleg Prezhdo − *Department of Chemistry and Department of Physics and Astronomy, University of Southern California, Los Angeles, California 90089, United States;* orcid.org/0000-0002-5140-7500

Dibyajyoti Ghosh − *Department of Chemistry and Department of Materials Science and Engineering (DMSE), Indian Institute of Technology, Delhi, New Delhi 110016, India;* orcid.org/0000-0002-3640-7537

Sergei A. Ivanov − *Materials Physics and Applications Division and Center for Integrated Nanotechnologies, Los Alamos National Laboratory, Los Alamos, New Mexico 87545, United States;* orcid.org/0000-0001-6790-5187

Complete contact information is available at: https://pubs.acs.org/10.1021/acs.chemmater.3c01414

Author Contributions

The manuscript was written through contributions of all authors. All authors have given approval to the final version of the manuscript. The authors declare no competing financial interest.

Notes

The authors declare no competing financial interest.

ACKNOWLEDGMENTS

The work at Los Alamos National Laboratory (LANL) was supported by the Laboratory Directed Research and Development (LDRD) Program at LANL under project 20200213DR. This work was done in part at the Center for Nonlinear Studies (CNLS) and the Center for Integrated Nanotechnologies (CINT), a U.S. Department of Energy and Office of Basic Energy Sciences user facility at LANL. This research used resources provided by the LANL Institutional Computing Program. Los Alamos National Laboratory is operated by Triad National Security, LLC, for the National Nuclear Security Administration of the U.S. Department of Energy (Contract No. 89233218NCA000001). D.G. acknowledges the IIT Delhi SEED Grant (PLN12/04MS) for support. O.V.P. acknowledges the support of the US Department of Energy, grant No. DE-SC0014429. S.K. acknowledges the support of the National Science Foundation under grant No. 2004197. For computational resources, this work used resources of the Center for Computationally Assisted Science and Technology (CCAST) at North Dakota State University, which were made possible in part by NSF MRI Award No. 2019077. All authors thank Dr. Victor I. Klimov for fruitful discussions.

REFERENCES

(1) Park, Y.-S.; Roh, J.; Diroll, B. T.; Schaller, R. D.; Klimov, V. I. Colloidal Quantum Dot Lasers. *Nat. Rev. Mater.* **2021**, *6*, 382−401.

(2) Jiang, Y.; Weiss, E. A. Colloidal Quantum Dots as Photocatalysts for Triplet Excited State Reactions of Organic Molecules. *J. Am. Chem. Soc.* **2020**, *142*, 15219−15229.

(3) Aznar-Gadea, E.; Rodriguez-Canto, P. J.; Albert Sanchez, S.; Martinez-Pastor, J. P.; Abargues, R. Luminescent CdSe Quantum Dot Arrays for Rapid Sensing of Explosive Taggants. *ACS Appl. Nano Mater.* **2022**, *5*, 6717−6725.

(4) Jurado-Sánchez, B.; Escarpa, A.; Wang, J. Lighting up Micromotors with Quantum Dots for Smart Chemical Sensing. *Chem. Commun.* **2015**, *51*, 14088−14091.

(5) Shivaji, K.; Mani, S.; Ponmurugan, P.; De Castro, C. S.; Davies, M. L.; Balasubramanian, M. G.; Pitchaimuthu, S. Green-Synthesis-Derived CdS Quantum Dots Using Tea Leaf Extract: Antimicrobial, Bioimaging, and Therapeutic Applications in Lung Cancer Cells. *ACS Appl. Nano Mater.* **2018**, *1*, 1683−1693.

(6) Kagan, C. R.; Bassett, L. C.; Murray, C. B.; Thompson, S. M. Colloidal Quantum Dots as Platforms for Quantum Information Science. *Chem. Rev.* **2021**, *121*, 3186−3233.

(7) Bharathi M, V.; Roy, N.; Moharana, P.; Ghosh, K.; Paira, P. Green Synthesis of Highly Luminescent Biotin-Conjugated CdSe Quantum Dots for Bioimaging Applications. *New J. Chem.* **2020**, *44*, 16891−16899.

(8) Ghosh, D.; Ivanov, S. A.; Tretiak, S. Structural Dynamics and Electronic Properties of Semiconductor Quantum Dots: Computational Insights. *Chem. Mater.* **2021**, *33*, 7848−7857.

(9) Goswami, P. N.; Mandal, D.; Rath, A. K. The Role of Surface Ligands in Determining the Electronic Properties of Quantum Dot Solids and Their Impact on Photovoltaic Figure of Merits. *Nanoscale* **2018**, *10*, 1072−1080.

(10) Zhou, J.; Liu, Y.; Tang, J.; Tang, W. Surface Ligands Engineering of Semiconductor Quantum Dots for Chemosensory and Biological Applications. *Mater. Today* **2017**, *20*, 360−376.

(11) Voznyy, O. Mobile Surface Traps in CdSe Nanocrystals with Carboxylic Acid Ligands. *J. Phys. Chem. C* **2011**, *115*, 15927−15932.

(12) Zeng, Y.; Kelley, D. F. Surface Charging in CdSe Quantum Dots: Infrared and Transient Absorption Spectroscopy. *J. Phys. Chem. C* **2017**, *121*, 16657−16664.

(13) Morris-Cohen, A. J.; Malicki, M.; Peterson, M. D.; Slavin, J. W. J.; Weiss, E. A. Chemical, Structural, and Quantitative Analysis of the Ligand Shells of Colloidal Quantum Dots. *Chem. Mater.* **2013**, *25*, 1155−1165.

(14) Swenson, N. K.; Ratner, M. A.; Weiss, E. A. Computational Study of the Influence of the Binding Geometries of Organic Ligands on the Photoluminescence Quantum Yield of CdSe Clusters. *J. Phys. Chem. C* **2016**, *120*, 6859−6868.

(15) Morris-Cohen, A. J.; Frederick, M. T.; Lilly, G. D.; McArthur, E. A.; Weiss, E. A. Organic Surfactant-Controlled Composition of the Surfaces of CdSe Quantum Dots. *J. Phys. Chem. Lett.* **2010**, *1*, 1078−1081.

(16) Sowers, K. L.; Hou, Z.; Peterson, J. J.; Swartz, B.; Pal, S.; Prezhdo, O.; Krauss, T. D. Photophysical Properties of CdSe/CdS Core/Shell Quantum Dots with Tunable Surface Composition. *Chem. Phys.* **2016**, *471*, 24−31.

(17) Wei, H. H.-Y.; Evans, C. M.; Swartz, B. D.; Neukirch, A. J.; Young, J.; Prezhdo, O. V.; Krauss, T. D. Colloidal Semiconductor Quantum Dots with Tunable Surface Composition. *Nano Lett.* **2012**, *12*, 4465−4471.

(18) Huang, M.-Y.; Li, X.-B.; Gao, Y.-J.; Li, J.; Wu, H.-L.; Zhang, L.-P.; Tung, C.-H.; Wu, L.-Z. Surface Stoichiometry Manipulation Enhances Solar Hydrogen Evolution of CdSe Quantum Dots. *J. Mater. Chem. A* **2018**, *6*, 6015−6021.

(19) Margraf, J. T.; Ruland, A.; Sgobba, V.; Guldi, D. M.; Clark, T. Theoretical and Experimental Insights into the Surface Chemistry of Semiconductor Quantum Dots. *Langmuir* **2013**, *29*, 15450−15456.
(20) Shim, M.; Guyot-Sionnest, P. N-Type Colloidal Semiconductor Nanocrystals. *Nature* **2000**, *407*, 981−983.
(21) Honarfar, A.; Mourad, H.; Lin, W.; et al. Photoexcitation Dynamics in Electrochemically Charged CdSe Quantum Dots: From Hot Carrier Cooling to Auger Recombination of Negative Trions. *ACS Appl. Energy Mater.* **2020**, *3*, 12525−12531.
(22) Wang, J. H.; Wang, L. F.; Yu, S. W.; Ding, T.; Xiang, D. M.; Wu, K. F. Spin Blockade and Phonon Bottleneck for Hot Electron Relaxation Observed in N-Doped Colloidal Quantum Dots. *Nat. Commun.* **2021**, *12* (1), No. 550.
(23) Azpiroz, J. M.; De Angelis, F. Ligand Induced Spectral Changes in CdSe Quantum Dots. *ACS Appl. Mater. Interfaces* **2015**, *7*, 19736−19745.
(24) Bhati, M.; Ivanov, S. A.; Senftle, T. P.; Tretiak, S.; Ghosh, D. Nature of Electronic Excitations in Small Non-Stoichiometric Quantum Dots. *J. Mater. Chem. A* **2022**, *10*, 5212−5220.
(25) Gai, Y. Q.; Peng, H. W.; Li, J. B. Electronic Properties of Nonstoichiometric PbSe Quantum Dots from First Principles. *J. Phys. Chem. C* **2009**, *113*, 21506−21511.
(26) Du Fossé, I.; Lal, S.; Hossaini, A. N.; Infante, I.; Houtepen, A. J. Effect of Ligands and Solvents on the Stability of Electron Charged CdSe Colloidal Quantum Dots. *J. Phys. Chem. C* **2021**, *125*, 23968−23975.
(27) Du Fossé, I.; ten Brinck, S.; Infante, I.; Houtepen, A. J. Role of Surface Reduction in the Formation of Traps in N-Doped II-VI Semiconductor Nanocrystals: How to Charge without Reducing the Surface. *Chem. Mater.* **2019**, *31*, 4575−4583.
(28) Jäger, M.; Schäfer, R. From Cd-Rich to Se-Rich − the Manipulation of CdSe Nanocluster Structure and Optical Absorption. *ChemPhysChem* **2021**, *22*, 192−196.
(29) Soloviev, V. N.; Eichhofer, A.; Fenske, D.; Banin, U. Size-Dependent Optical Spectroscopy of a Homologous Series of CdSe Cluster Molecules. *J. Am. Chem. Soc.* **2001**, *123*, 2354−2364.
(30) Kilina, S. V.; Tamukong, P. K.; Kilin, D. S. Surface Chemistry of Semiconducting Quantum Dots: Theoretical Perspectives. *Acc. Chem. Res.* **2016**, *49*, 2127−2135.
(31) Kilina, S.; Kilin, D.; Tretiak, S. Light-Driven and Phonon-Assisted Dynamics in Organic and Semiconductor Nanostructures. *Chem. Rev.* **2015**, *115*, 5929−5978.
(32) Makarov, N. S.; Guo, S.; Isaienko, O.; Liu, W.; Robel, I.; Klimov, V. I. Spectral and Dynamical Properties of Single Excitons, Biexcitons, and Trions in Cesium-Lead-Halide Perovskite Quantum Dots. *Nano Lett.* **2016**, *16*, 2349−2362.
(33) Park, Y.-S.; Bae, W. K.; Pietryga, J. M.; Klimov, V. I. Auger Recombination of Biexcitons and Negative and Positive Trions in Individual Quantum Dots. *ACS Nano* **2014**, *8*, 7288−7296.
(34) Akimov, I. A.; Flissikowski, T.; Hundt, A.; Henneberger, F. Spin Processes Related to Trions in Quantum Dots. *Phys. Status Solidi A* **2004**, *201*, 412−420.
(35) Henzler, P.; Traum, C.; Holtkemper, M.; et al. Femtosecond Transfer and Manipulation of Persistent Hot-Trion Coherence in a Single CdSe/ZnSe Quantum Dot. *Phys. Rev. Lett.* **2021**, *126* (6), No. 067402.
(36) Meng, L.; Wang, X. Doping Colloidal Quantum Dot Materials and Devices for Photovoltaics. *Energies* **2022**, *15*, 2458.
(37) Kirmani, A. R.; Kiani, A.; Said, M. M.; Voznyy, O.; Wehbe, N.; Walters, G.; Barlow, S.; Sargent, E. H.; Marder, S. R.; Amassian, A. Remote Molecular Doping of Colloidal Quantum Dot Photovoltaics. *ACS Energy Lett.* **2016**, *1*, 922−930.
(38) Greaney, M. J.; Couderc, E.; Zhao, J.; Nail, B. A.; Mecklenburg, M.; Thornbury, W.; Osterloh, F. E.; Bradforth, S. E.; Brutchey, R. L. Controlling the Trap State Landscape of Colloidal CdSe Nanocrystals with Cadmium Halide Ligands. *Chem. Mater.* **2015**, *27*, 744−756.
(39) Gumber, S.; Eniodunmo, O.; Ivanov, S. A.; Kilina, S.; Prezhdo, O. V.; Ghosh, D.; Tretiak, S. Hot Carrier Relaxation Dynamics in Non-Stoichiometric CdSe Quantum Dots: Computational Insights. *J. Mater. Chem. A* **2023**, *11*, 8256−8264.
(40) Tang, J.; et al. Colloidal-Quantum-Dot Photovoltaics Using Atomic-Ligand Passivation. *Nat. Mater.* **2011**, *10*, 765−771.
(41) Kim, W. D.; Kim, J. H.; Lee, S.; et al. Role of Surface States in Photocatalysis: Study of Chlorine-Passivated CdSe Nanocrystals for Photocatalytic Hydrogen Generation. *Chem. Mater.* **2016**, *28*, 962−968.
(42) Cui, Y.; Cui, X.; Zhang, L.; Xie, Y.; Yang, M. Theoretical Characterization on the Size-Dependent Electron and Hole Trapping Activity of Chloride-Passivated CdSe Nanoclusters. *J. Chem. Phys.* **2018**, *148*, No. 134308.
(43) van der Stam, W.; du Fosse, I.; Grimaldi, G.; Monchen, J. O. V.; Kirkwood, N.; Houtepen, A. J. Spectroelectrochemical Signatures of Surface Trap Passivation on CdTe Nanocrystals. *Chem. Mater.* **2018**, *30*, 8052−8061.
(44) Munro, A. M.; Chandler, C.; Garling, M.; Chai, D.; Popovich, V.; Lystrom, L.; Kilina, S. Phenyldithiocarbamate Ligands Decompose During Nanocrystal Ligand Exchange. *J. Phys. Chem. C* **2016**, *120*, 29455−29462.
(45) Homer, M. K.; Kuo, D.-Y.; Dou, F. Y.; Cossairt, B. M. Photoinduced Charge Transfer from Quantum Dots Measured by Cyclic Voltammetry. *J. Am. Chem. Soc.* **2022**, *144*, 14226−14234.
(46) Hartley, C. L.; Dempsey, J. L. Electron-Promoted X-Type Ligand Displacement at CdSe Quantum Dot Surfaces. *Nano Lett.* **2019**, *19*, 1151−1157.
(47) Fischer, S. A.; Crotty, A. M.; Kilina, S. V.; Ivanov, S. A.; Tretiak, S. Passivating Ligand and Solvent Contributions to the Electronic Properties of Semiconductor Nanocrystals. *Nanoscale* **2012**, *4*, 904−914.
(48) Jha, P. P.; Guyot-Sionnest, P. Trion Decay in Colloidal Quantum Dots. *ACS Nano* **2009**, *3*, 1011−1015.
(49) Louyer, Y.; Biadala, L.; Tamarat, P.; Lounis, B. Spectroscopy of Neutral and Charged Exciton States in Single CdSe/ZnS Nanocrystals. *Appl. Phys. Lett.* **2010**, *96*, No. 203111.
(50) Qin, W.; Liu, H.; Guyot-Sionnest, P. Small Bright Charged Colloidal Quantum Dots. *ACS Nano* **2014**, *8*, 283−291.
(51) Honarfar, A.; Chabera, P.; Lin, W.; Meng, J.; Mourad, H.; Pankratova, G.; Gorton, L.; Zheng, K.; Pullerits, T. Ultrafast Spectroelectrochemistry Reveals Photoinduced Carrier Dynamics in Positively Charged CdSe Nanocrystals. *J. Phys. Chem. C* **2021**, *125*, 14332−14337.
(52) Hinz, C.; Gumbsheimer, P.; Traum, C.; et al. Charge and Spin Control of Ultrafast Electron and Hole Dynamics in Single CdSe/ZnSe Quantum Dots. *Phys. Rev. B* **2018**, *97*, No. 045302.
(53) Jasieniak, J.; Mulvaney, P. From Cd-Rich to Se-Rich - the Manipulation of CdSe Nanocrystal Surface Stoichiometry. *J. Am. Chem. Soc.* **2007**, *129*, 2841−2848.
(54) Ramirez-Torres, A.; Turkowski, V.; Rahman, T. S. Time-Dependent Density-Matrix Functional Theory for Trion Excitations: Application to Monolayer MoS2 and Other Transition-Metal Dichalcogenides. *Phys. Rev. B* **2014**, *90*, No. 085419.
(55) Turkowski, V.; Din, N. U.; Rahman, T. S. Time-Dependent Density-Functional Theory and Excitons in Bulk and Two-Dimensional Semiconductors. *Computation* **2017**, *5*, 39.
(56) Frisch, M. J. et al. *Gaussian 16*, Revision B.01; Gaussian, Inc.: Wallingford, CT, USA, 2016.
(57) Becke, A. D. Density-functional thermochemistry. I. The effect of the exchange-only gradient correction. *J. Chem. Phys.* **1993**, *98*, 2155−2160.
(58) Hay, P. J.; Wadt, W. R. Abinitio Effective Core Potentials for Molecular Calculations - Potentials for the Transition-Metal Atoms Sc to Hg. *J. Chem. Phys.* **1985**, *82*, 270−283.
(59) Ditchfield, R. H.; Hehre, W. J.; Pople, J. A. Self-Consistent Molecular-Orbital Methods. 9. Extended Gaussian-Type Basis for Molecular-Orbital Studies of Organic Molecules. *J. Chem. Phys.* **1971**, *54*, 724−728.
(60) Martin, R. L. Natural Transition Orbitals. *J. Chem. Phys.* **2003**, *118*, 4775−4777.

(61) Lüftner, D.; Ules, T.; Reinisch, E. M.; Koller, G.; Soubatch, S.; Tautz, F. S.; Ramsey, M. G.; Puschnig, P. Imaging the Wave Functions of Adsorbed Molecules. *Proc. Natl. Acad. Sci. U.S.A.* **2014**, *111* (2), 605−610.
(62) Lu, T.; Chen, F. Multiwfn: A Multifunctional Wavefunction Analyzer. *J. Comput. Chem.* **2012**, *33*, 580−592.
(63) Humphrey, W.; Dalke, A.; Schulten, K. VMD: Visual Molecular Dynamics. *J. Mol. Graphics* **1996**, *14*, 33−38.
(64) Cossi, M.; Rega, N.; Scalmani, G.; Barone, V. Energies, Structures, and Electronic Properties of Molecules in Solution with the C-Pcm Solvation Model. *J. Comput. Chem.* **2003**, *24*, 669−681.
(65) Albert, V. V.; Ivanov, S. A.; Tretiak, S.; Kilina, S. V. Electronic Structure of Ligated CdSe Clusters: Dependence on DFT Methodology. *J. Phys. Chem. C* **2011**, *115*, 15793−15800.
(66) Lystrom, L.; Roberts, A.; Dandu, N.; Kilina, S. Surface-Induced Deprotonation of Thiol Ligands Impacts the Optical Response of CdS Quantum Dots. *Chem. Mater.* **2021**, *33*, 892−901.

https://doi.org/10.1021/acs.chemmater.3c01414
Chem. Mater. 2024, 36, 146−156